JOURNAL OF MATERIALS SCIENCE 29 (1994) 5934–5946

Preparation of ceramic coatings from pre-ceramic precursors

Part II *SiC on metal substrates*

M. R. MUCALO*, N. B. MILESTONE
Materials Science and Performance (MSP) Group, The New Zealand Institute for Industrial Research and Development (Industrial Research Ltd), P.O. Box 31-310, Lower Hutt, New Zealand

SiC-coatings derived from pyrolysis of polycarbosilane layers on stainless steel and mild steel substrates have been studied using a combination of scanning electron microscopy (SEM), energy dispersive X-ray analysis, X-ray photoelectron spectroscopy and ultramicrohardness techniques. The coatings on mild steel plates at firing temperatures of 700 °C are cracked but uncracked SiC coatings can be formed on stainless steel substrates at 700–800 °C. X-ray photoelectron studies show that these coatings are covered with a layer of SiO_2 and contain graphitic carbon, while Rutherford backscattering studies indicate inhomogeneities in the coating layer due to mixing of substrate and coating components at the interface between the two. Ultramicrohardness results indicate the SiC/stainless steel coatings formed at 800 °C are softer than the equivalent SiC coatings formed on alumina substrates at 1100 °C. Above 800 °C, a possible combination of both thermal expansion mismatch and CrN formation, which causes the growth of chromium-rich nodules in the stainless steel, serve to disrupt and ultimately destroy the coherence of the SiC coatings. The use of sol–gel-derived SiO_2 coatings as a barrier does not prevent the destruction of the SiC coating by this mechanism.

1. Introduction

In Part I of this study [1], it was shown that crack-free coatings of SiC and Si_3N_4 can be formed on alumina, silicon and silica plates by 1100 °C-N_2 pyrolyses of applied polycarbosilane (PCS) and poly(diphenyl) silazane (PDPS) layers. The objectives of this research were to devise methods of forming coatings derived from pyrolyses of PCS and PDPS on substrates for potential use in wear and corrosion resistance in industry. Accordingly, it was decided to extend the study to include metal substrates which could benefit from any increased corrosion resistance that the application of these coatings may offer.

There is not a great volume of work involving metal/pre-ceramic polymer systems. Yajima *et al.* [2] produced a new sintered alloy by coating particles of Fe–13Cr with polycarbosilane. Heating of the mixture led to the formation of fine grains of amorphous SiC dispersed uniformly in the alloy which exhibited greater hardness and wear resistance at both high and room temperatures and large corrosion resistance at high temperatures. Seyferth *et al.* [3] pyrolysed pre-ceramic polymer/metal powder composites (e.g. W/PCS) to form ceramic products which contained crystalline phases of metal silicides (e.g. WSi_2, W_5Si_3), metal carbides, metal nitrides, metal borides and silicon carbide.

However, research on polymer-derived coatings on planar metal substrates seems to be lacking. This paper explores the conditions necessary for forming coherent PCS-derived SiC coatings on stainless steel and mild steel plates using the same array of techniques (SEM/energy dispersive X-ray analysis, X-ray photoelectron spectroscopy, Rutherford backscattering, ultramicrohardness) as in Part I of this study [1].

2. Experimental procedure

2.1. Preparation of pre-ceramic polymers

Polycarbosilane (PCS) was prepared as described in Part I [1] from heating of poly(dimethyl)silane (PDMS) powder to 470 °C under argon in a pressurized stainless steel bomb. Poly(diphenyl)silazane (PDPS) was produced [1] by NH_4Br-catalysed polymerization of the phenylsilazane oil obtained from ammonolysis of $(C_6H_5)_2SiCl_2$.

* Author to whom all correspondence should be addressed. *Present address*: STA Fellow, Government Industrial Research Institute, Nagoya, 1-1 Hirate-cho, Kita-ku, Nagoya City, Aichi Pref. 462, Japan.

0022–2461

2.2. Preparation of coating solutions and metal substrates

2.2.1. Metal plates and cleaning procedure

Small rectangular plates were cut from industrial stainless steel and mild steel sheet. Two types of stainless steel were used: because the stainless steel type was not available, the samples were characterized by EDX. The first type, referred to as "SSI", exhibited the following normalized elemental per cent (el %) values from EDX analysis: Si (0.472), Cr (16.941), Mn (0.572), Fe (72.666) and Ni (9.117). Normalized el % values for the second type of stainless steel "SS2" were Si (0.451), Mo (2.028), Cr (15.970), Mn (1.455), Fe (68.235) and Ni (11.861) while those for the mild steel plate were Fe (99.445), Si (0.226) and Mn (0.329). These analyses were referenced to a cobalt standard. However, given that the detector used for the EDX analyses can only measure elements above sodium, it is likely that other lower atomic weight components (e.g. boron in "SS1" and carbon in mild steel) are present in the metal plates.

Mild steel plates were initially dipped in aqua regia prior to a thorough rinse in water, drying and storage under nujol until required. Both stainless steel and mild steel plates were ultrasonically cleaned prior to coating in a degreasing surfactant (DECON)/water solution and then rinsed in water and A.R. grade acetone followed by drying in an oven.

2.2.2. Preparation of coating solutions

60%–70% (wt/vol) PCS coating solutions were prepared by the dissolution of pre-weighed amounts of PCS in measured volumes of *n*-hexane.

The sol–gel SiO_2 coating solution was prepared following the procedure reported by Pope and McKenzie [4]. 19.69 g ethyl silicate (TEOS), 17.39 g absolute ethanol, 6.83 g distilled water and 0.31 g glacial acetic acid were weighed into a glass jar and mixed by swirling to effect miscibility. The jar was then covered with semi-permeable plastic and the solution allowed to age. After standing overnight, the solution was used for coating for 4 days following its preparation.

2.2.3. Coating methods

All metal substrates were dip-coated in small troughs of coating solution using a special in-house constructed dip-coater described in Part I of this study [1]. All dip-coating was conducted at 4 cm min^{-1}. The following system of nomenclature was used for SiO_2 coating of substrates using the sol–gel solution prepared as a function of age of the coating solution.

"1,1" plate = one (1) layer of SiO_2 formed by dip-coating in a sol–gel coating solution on the first (1) day after its preparation (hence "1,1").
"1,2" plate = one (1) layer of SiO_2 formed by dip-coating in a sol–gel coating solution on the second (2) day after its preparation.
"1,3" plate = one (1) layer of SiO_2 formed by dip-coating in a sol–gel coating solution three (3) days after its preparation.
"1,4" plate = one (1) layer of SiO_2 formed by dip-coating in a sol–gel coating solution four (4) days after its preparation.
"1,1,2,2" = as for "1,1" then a second (2) layer of SiO_2 formed by dipping the "1,1" plate in the sol–gel SiO_2 coating solution on the second (2) day after its preparation.

2.3. Pyrolyses

All pyrolyses were conducted in a temperature-programmed alumina tube furnace under flowing nitrogen or argon (100–200 ml min^{-1}). For metal plates heated to 700–850 °C, heating to 600–650 °C was initially carried out at 5 °C min^{-1} after which slow heating at 1 °C min^{-1} to the final pyrolysis temperature was carried out. For 900 °C pyrolyses, heating at 1 °C min^{-1} was commenced when the temperature had reached 700 °C. 1100 °C pyrolyses were conducted using an overall heating rate of 2 °C min^{-1} to the maximum pyrolysis temperature. For all pyrolyses, the temperature of the tube furnace was held at the maximum pyrolysis temperature for 1–2 h before being allowed to cool.

Sol–gel-derived SiO_2 coatings were prepared by heating dip-coated metal plates at 2.5 °C min^{-1} to 500 °C at which samples were held for 1 h prior to cooling.

2.4. Instrumentation

Scanning electron micrographs and energy dispersive X-ray analyses (EDX) were obtained on a Cambridge Stereoscan 250 Mk II electron microscope which employed a Link 860 Series 2 computing system. Samples examined were usually carbon-coated or gold–palladium-coated. EDX analyses of carbon-coated samples were conducted at 10 or 20 kV. Specimens smaller than 2 cm diameter were examined by a Philips PD1700 APD X-ray diffractometer with a diffracted beam monochromator and automatic divergence slit. Larger samples were examined using a microprocessor-controlled Philips X-ray Diffraction instrument with a PW1050 goniometer, graphite-diffracted monochromator and a fixed divergence slit. CoK_α radiation was employed in both XRD instruments. X-ray photoelectron spectra were recorded on a Kratos XSAM 800 X-ray Photoelectron Spectrometer using a DS800 data system. Wide scans were acquired over the 0–900 eV region using non-monochromatized MgK_α radiation of samples attached to stainless steel sample stubs by means of double-sided sticky tape. Binding energy shifts observed in spectra due to sample charging were usually referenced to the binding energy shift of C 1s (284.8 eV) [5] due to adventitious hydrocarbons. Narrow scans were recorded using non-monochromatized X-ray radiation using an electron pass energy of 20 eV over the C 1s (280–295 eV), O 1s (530–550 eV), and Si 2p (90–115 eV) regions of the X-ray photoelectron spectra of specimens.

Rutherford backscattering spectrometry (RBS) was carried out on SiC-coated and uncoated stainless steel

samples in the new ion beam analysis (IBA) facility at the Institute of Geological and Nuclear Sciences Ltd. Experimental conditions for these experiments have been described in Part I [1]. As described earlier [1], RBS spectra were interpreted by fitting with RUMP [6], using assumed concentration profiles and "fuzzing" [7] to account for the roughness at the substrate/coating interface.

The microhardness of coatings formed in this study was measured using a UMIS-2000 (ultra micro-indentation system) instrument developed [8, 9] at the CSIRO Division of Applied Physics in New South Wales, Australia. Load–unload plots were obtained using loads of 500, 200, 100, 50, 20, 10 and 5 mN on coated and uncoated stainless steel specimens. Typically, at least six separate micro-indentations were made for each load at selected sites throughout the surface and the results averaged. Indentations were made with the use of a triangular diamond pyramid Berkovich indentor. The indentations in the coatings were examined using SEM in order to gain some understanding of the adhesive and delamination performance of the coating under study.

All ^{29}Si magic angle spinning (MAS) nuclear magnetic resonance (NMR) spectra of bulk pyrolytic material generated were recorded using a Varian Unity 500 solid state NMR spectrometer. 12–16 transients (acquisition time of each transient, 0.041 s) were obtained from powdered pyrolytic residues spun in zirconia rotors. 90° pulse widths were of the order of 5.5 μs with delay times between successive transients of 30 or 300 s. Line-broadening factors of 200–400 Hz were normally applied in spectral processing.

3. Results and discussion

3.1. Studies of PCS-derived SiC coatings formed at 700–1100 °C on mild steel and stainless steel substrates

In Part I it was demonstrated that PCS-derived SiC and PDPS-derived "Si_3N_4/Si_2N_2O" multilayers could be formed successfully on alumina, silicon and silica substrates at pyrolysis temperatures of 1100 °C in nitrogen [1]. In the present study, PCS layers applied by spin- or dip-coating on stainless steel and mild steel substrates were initially pyrolysed to 1100 °C in nitrogen with the desire of achieving the same result as with the SiC/alumina systems (see later). However, this initial approach resulted in problems arising from various factors involving the substrate and the coating material, so coating formation was studied as a function of pyrolysis temperature starting at 700 °C.

The lower limit of 700 °C was chosen on the basis of a solid-state NMR study by Taki *et al.* [10] where the conversion process of PCS to amorphous SiC was reported to begin at 600 °C and be essentially complete between 700 and 1000 °C. Pyrolyses were conducted in a furnace programmed to heat at 5 °C min^{-1} to 600 °C followed by a slower heating rate of 1 °C min^{-1} from 600 °C to 700, 800, 850 or 900 °C to allow the conversion of PCS to SiC to occur.

In order to characterize the coating material being formed on the metal substrates at the lower temperatures of 700 and 800 °C, samples of bulk PCS were pyrolysed at 700 and 800 °C in nitrogen and the residues examined by ^{29}Si MAS NMR spectroscopy. Both spectra were practically identical in appearance to the spectrum reported by Taki *et al.* [10] for the PCS-derived residue pyrolysed to 700 °C. NMR analysis of the 700 °C-N_2 pyrolysis residue in the present study appeared to contain a small amount of Si–O character as evident from a rather weak peak observed at approximately −90 to −95 p.p.m. which has been associated with SiO_2-type species [11].

3.1.1. SEM/EDX studies of SiC-coated stainless steel and mild steel plates at 700–1100 °C

3.1.1.1. Coatings formed on Mild Steel Plates. (i)700 °C. The first coating of PCS-derived SiC on mild steel plates after application of PCS by dip-coating followed by 700 °C-N_2 pyrolysis was a golden-brown colour. Subsequent coatings were black. The EDX-derived plot of at % (Si)/at % (Fe) versus number of SiC layers (see Fig. 1) gave an approximately linear plot with positive slope indicating accumulation of coating material on the substrate without loss by spalling between separate pyrolyses. SEM, however (see Fig. 2) showed that for all plates (with one to four layers of SiC) cracking was present in all coatings. Nevertheless, spot EDX analyses of plates with two or more coatings indicated that there was no point where the cracks extended through to the substrate. Although spalling was not apparent on the coated specimens, the extensive variation of Si/Fe ratios on the same sample was an indication that the coatings were rather non-uniform in thickness which is likely to be a consequence of the rather severe cracking.

(ii) 1100 °C. Given the results of coating formation at 700 °C, it is not surprising that 1100 °C-N_2 pyrolysis of PCS directly applied to mild steel plates is not successful. When such samples were examined by SEM, a coating was either not readily apparent or was catastrophically cracked. The failure of coating formation on the mild steel substrate may be due to reaction of the nascent SiC coating with mild steel (see later). An additional problem is the mismatch of thermal expansion coefficient, α, between the substrate and

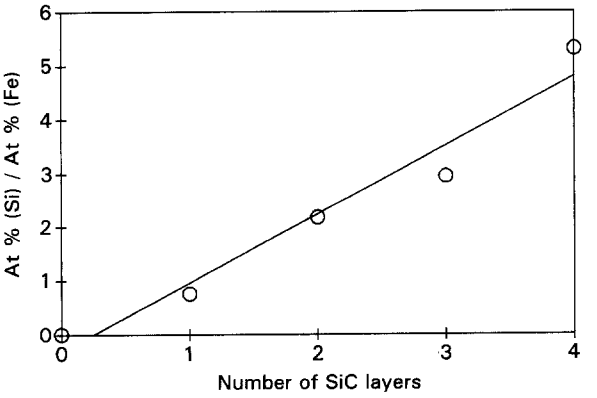

Figure 1 Plot of at % (Si)/at % (Fe) against the number of applied SiC layers from EDX-derived data for SiC formed on mild steel plates at 700 °C.

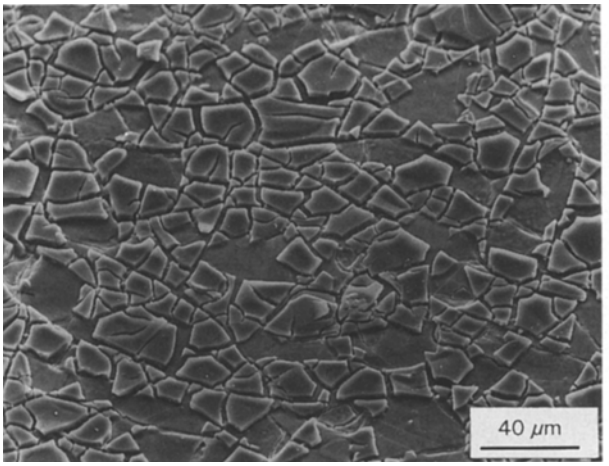

Figure 2 Scanning electron micrograph of a mild steel plate coated with three SiC layers.

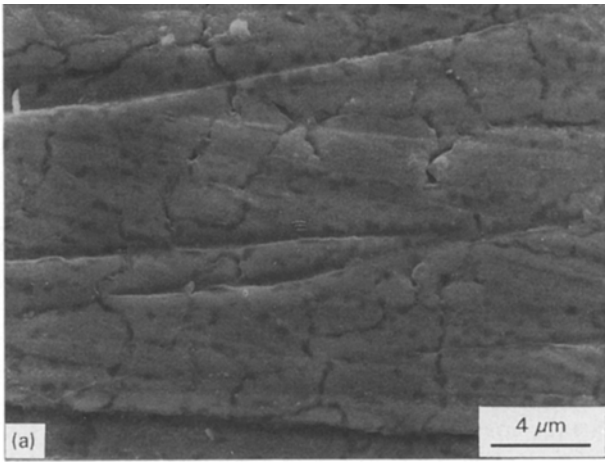

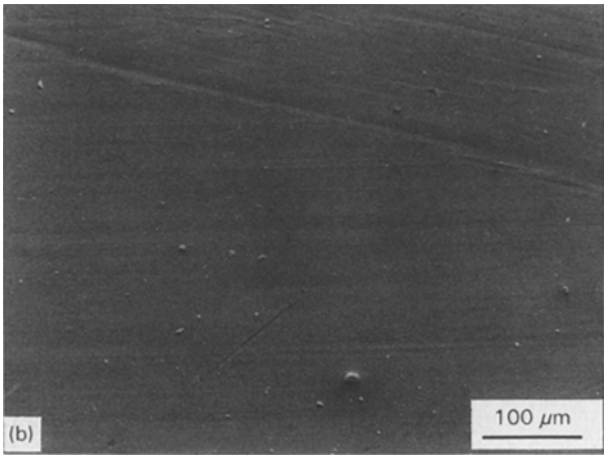

Figure 3 Scanning electron micrographs of SiC layers deposited on stainless steel plates at 700 °C: (a) one layer of SiC, and (b) three layers of SiC.

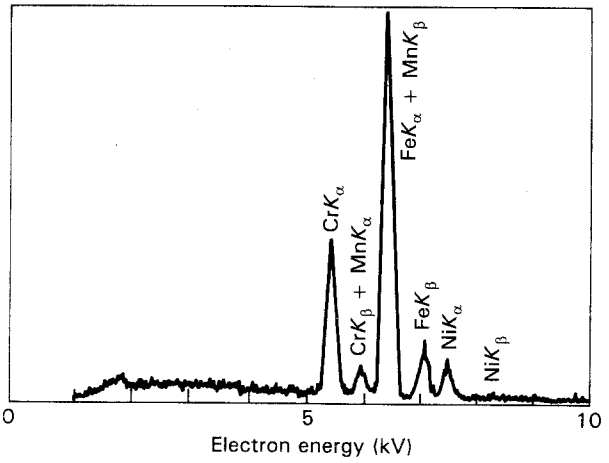

Figure 4 Typical EDX spectrum of as-received stainless steel sheet.

the SiC coating. Mild steel exhibits α values of 10–$20 \times 10^{-6}\,°C^{-1}$ [12] while pyrolytic SiC exhibits α values of $4.4–4.6 \times 10^{-6}\,°C^{-1}$ [13]. This large mismatch could be a major reason for the degree of cracking observed in SiC coatings formed at 700 °C on mild steel substrates.

3.1.1.2. Coatings formed on stainless steel at 700–900 °C. "SS1" and "SS2" were indistinguishable as substrates on which PCS-derived SiC coatings were deposited. The differences between the two substrates only became evident during XPS analysis (see later).

(i) 700 °C. The first layer of PCS-derived SiC after 700 °C-N_2 pyrolysis of a dip-coated layer of PCS on stainless steel was also golden-brown. The first layer of SiC deposited at 700 °C was extremely thin, because when examined by SEM, grain boundaries of the stainless steel plate could still be seen through the coating (see Fig. 3a). Coating thickness could, however, be built up on the plates by repeated dip-coating and pyrolyses. By the third layer, a dark brown sheen was apparent on the stainless steel plates. The scanning electron micrograph of such a coating (see Fig. 3b) revealed no cracking.

The typical EDX pattern for the stainless steel substrate was found to be sensitive to adverse changes occurring in the coatings and was thus useful as an indicator for the overall success of forming coatings on the plates from pre-ceramic precursors. Thus, for the coatings formed by 700 °C-N_2 pyrolysis, the EDX of the stainless steel was identical to the typical pattern for an unheated, uncoated plate (see Fig. 4). Given that the SEM showed crack-free coatings, this indicates that coating formation has been reasonably successful at this pyrolysis temperature.

(ii) 800 °C. Repeated dip-coatings and 800 °C pyrolyses allowed the deposition of multilayers of SiC on the plates as in the case for the coatings formed at 700 °C. The coatings were darker in colour than those formed at 700 °C. A black sheen had developed by the third coating. A scanning electron micrograph recorded of three SiC layers formed at 800 °C on stainless steel revealed a smooth, uncracked coating although substrate-associated features such as scratches were also evident. In addition, the EDX signals of the stainless steel substrate were unchanged in appearance from Fig. 4. Thus, it is evident that PCS-derived layers can also be successfully formed on stainless steel substrates by 800 °C-N_2 pyrolyses.

A method employed for determining the approximate coating thicknesses of the crack-free coatings of PCS-derived SiC at 700–800 °C was similar to that

employed for determining coating thicknesses of SiC and "Si_3N_4/Si_2N_2O" coatings on alumina plates in an earlier study [1]. In the present study, the SEM excitation voltage at which the chromium and iron signals just disappeared from the EDX spectrum was taken as the point at which only the coating was being viewed by SEM. Unlike the SiC/alumina coating system, this was found to be a more difficult exercise as the FeK_α and CrK_α peaks occurred on a sloping baseline.

The Kanaya equation [14] was used to determine coating thickness as used for SiC coatings on alumina plates [1]. Coating thicknesses were found to be low for the coated specimens examined. For four layers of PCS-derived SiC formed on stainless steel plates at 700 °C, the thickness was calculated to be ~ 630 nm. In the case of coatings formed at 800 °C, coating thickness was similar at 580 nm for four layers of SiC. The thin layers formed would explain why substrate-associated features are still visible through the coatings by SEM as coating formation build up.

(iii) 850, 900 °C. PCS layers on stainless steel plates applied by dip-coating were pyrolysed to temperatures of 850–900 °C in a desire to produce harder coatings than those formed at 700–800 °C. A single coat of SiC formed on a stainless steel at 850 °C was similar in appearance to the shiny, black coatings formed at 800 °C. However, electron micrographs of SiC coatings formed at 850 °C revealed that shallow cracks had begun to develop in the coatings (see Fig. 5a). Electron micrographs with similar features were observed for coatings formed at 900 °C. Fig. 5b is a micrograph of a typical cracked region in the coating formed at 900 °C.

EDX spectra of the coated, uncoated and cracked regions of SiC coatings formed at 850–900 °C on stainless steel are illustrated in Fig. 6. In uncracked coated regions, the substrate-associated peaks in the EDX spectrum (Fig. 6a) were mostly unchanged relative to the spectrum in Fig. 4. However, in the uncoated region of the plate (Fig. 6b), the EDX spectra showed significant enhancements in intensity for the CrK_α and MnK_α peaks due to migration of chromium and manganese in the stainless steel. Migration of stainless steel components, notably chromium is probably caused by the tendency of this element to become nitrided in the nitrogen atmosphere. This was confirmed in XPS results (see later). In addition, previous authors have shown that chromium and molybdenum can form interstitial nitrides on stainless steel in case-hardening experiments [15]. Migration of other elements typically contained in stainless steel (namely manganese or silicon) may form a tenacious barrier oxide layer on the substrate surface in response to the high temperatures to which the stainless steel is subjected [16, 17]. The relatively unchanged appearance of the EDX spectrum in Fig. 6a is an indication that the SiC coating is providing some thermal protection to the stainless steel plate.

The EDX spectrum (Fig. 6c) of the nodules and dimples in and around the crack illustrated in Fig. 5b showed that they were strongly enriched in chromium and manganese. This lends support to CrN formation

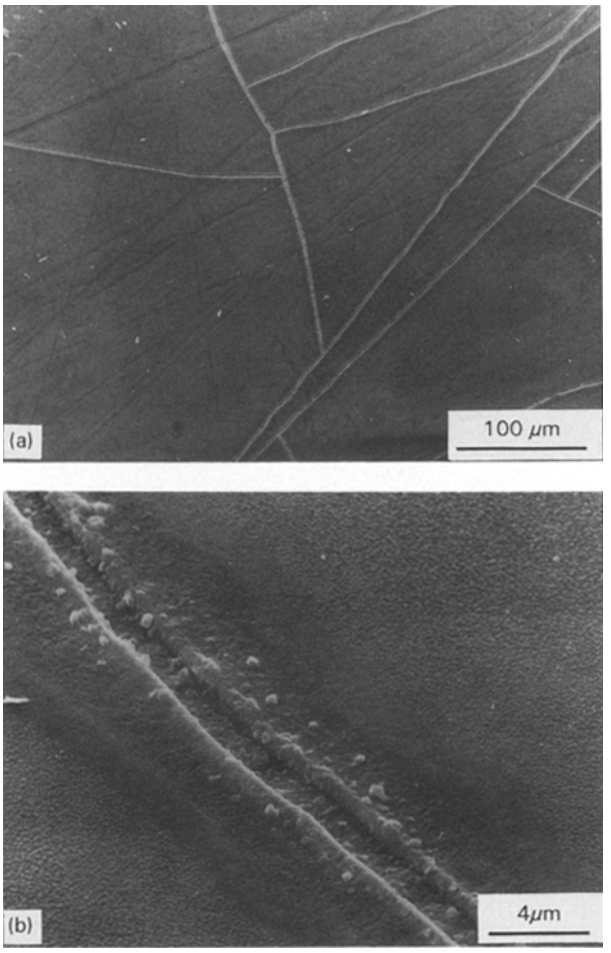

Figure 5 Scanning electron micrographs of (a) coating of SiC on stainless steel formed at 850 °C and (b) in the vicinity of cracked region of SiC coating on stainless steel formed at 900 °C.

(as well as possibly MnO_2 formation) being a cause for the emergence of cracks in the SiC coating at 850–900 °C.

(iv) 1100 °C. In order to harden the SiC coatings, a stainless steel plate with four layers of PCS-derived SiC pre-deposited at 700 °C was heated to 1100 °C in nitrogen. SEM (Fig. 7a) indicated that the coating had cracked and become totally disrupted as a result of the 1100 °C-N_2 pyrolysis. EDX analysis indicated a significant change in the relative intensities of the components of stainless steel with the CrK_α and MnK_α peaks showing substantial increases in intensity. Because the success of coating in many instances is indirectly indicated by the lack of change in the EDX stainless steel peaks, it is obvious that substrate-associated processes which were causing mild cracking at 850–900 °C serve to destroy completely coating coherency at 1100 °C.

To gain a better understanding of how the substrate *per se* behaves at high temperatures, an uncoated stainless steel plate was heated under identical conditions to those used for forming SiC on stainless steel plates (1100 °C, flowing nitrogen). After heating, the initial sheen of the stainless steel plate had disappeared and was replaced by a rather dull grey matt appearance. SEM (Fig. 7b) showed that the surface of the plate had become considerably roughened with a

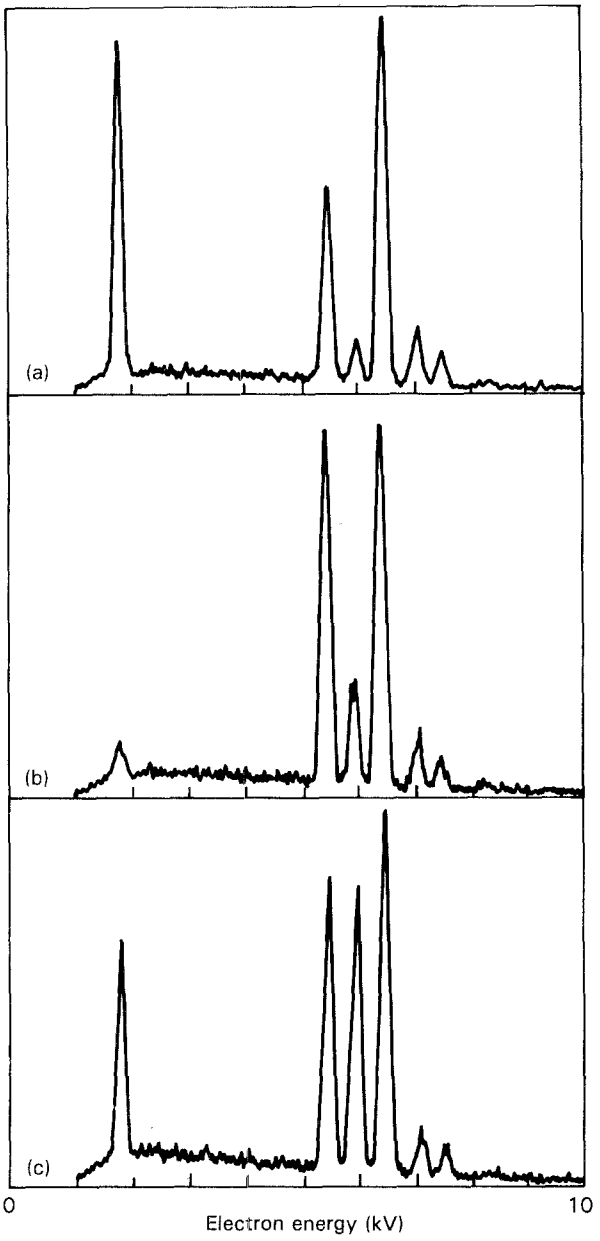

Figure 6 EDX spectra of SiC coatings formed on stainless steel formed at 850 and 900 °C: (a) uncracked, coated area, (b) uncoated area of plate, and (c) region containing dimples and nodules in and around the coating crack.

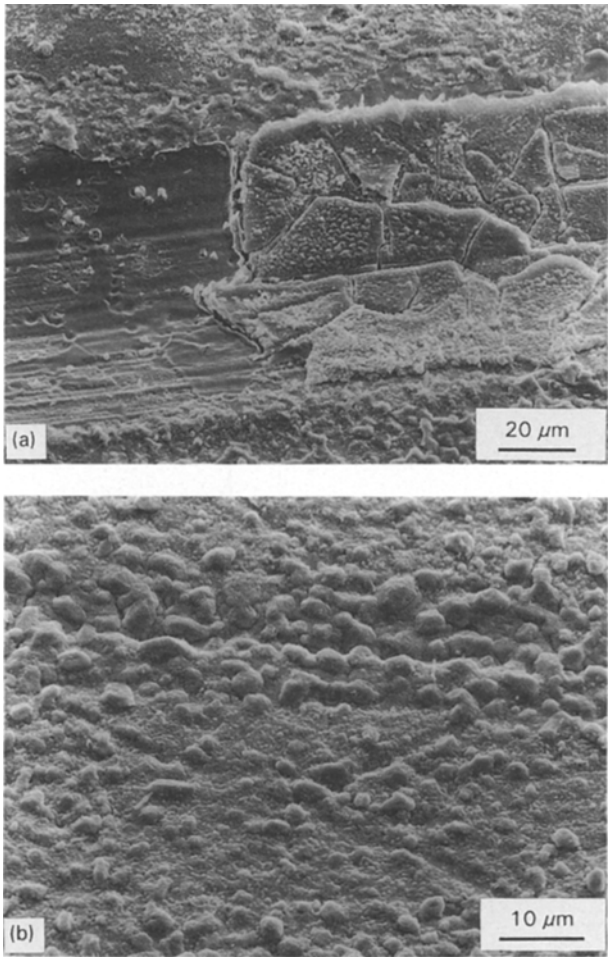

Figure 7 Scanning electron micrographs of (a) stainless steel predeposited with four layers of SiC at 700 °C, heated to 1100 °C in nitrogen and (b) uncoated stainless steel plate heated to 1100 °C in nitrogen.

significant number of lumps or nodules interspersed throughout the surface. A spot EDX analysis indicated that the nodules were highly enriched in chromium while analysis over a wider area showed enhanced chromium and manganese levels. Given that XPS analysis (see later) shows that the surface of the stainless steel plates has been nitrided, it is likely that the raised lumps are CrN. Previous workers have shown by XPS of nitrogen-implanted austenitic stainless steels that chromium-rich nitrides form as islands in the passive film [18]. The formation of the CrN nodules probably contribute to coating failure at temperatures above 850 °C by slowly emerging from the substrate creating fissures or breaking through weak spots in the SiC coating. This would lead to catastrophic cracking of coatings at higher temperatures (e.g. 1100 °C). This is supported by the EDX analyses conducted in cracks appearing in coatings formed at 850 °C (see above) which showed increased levels of chromium at the surface and around cracks.

3.1.1.3. Use of argon as the pyrolysis flow gas. When a stainless steel plate initially coated with three layers of PCS-derived SiC formed by separate 700 °C-Ar pyrolyses, was heated to 1100 °C also in argon, the SiC multilayers did not survive the 1100 °C firing. The plate had an all-over grey appearance and micrographs of the coated plates indicated that the SiC coats were extremely disrupted. However, the stainless steel-associated EDX peaks (see Fig. 8a) on the coated plates were only slightly altered (with a slight enhancement in the CrK_α peak, see Fig. 4 for identification of EDX peaks) as a result of the 1100 °C firing in argon. In contrast, the EDX spectrum for an uncoated stainless steel plate heated to 1100 °C in argon (Fig. 8b) indicated a significant migration of chromium and manganese as well as the silicon which was present in the stainless steel. The lack of change observed in the EDX (Fig. 8a) of the coated plate suggested that the SiC coating, despite being disrupted, still provided thermal protection to the stainless steel relative to an uncoated plate subjected to identical conditions. Such thermal protection was also

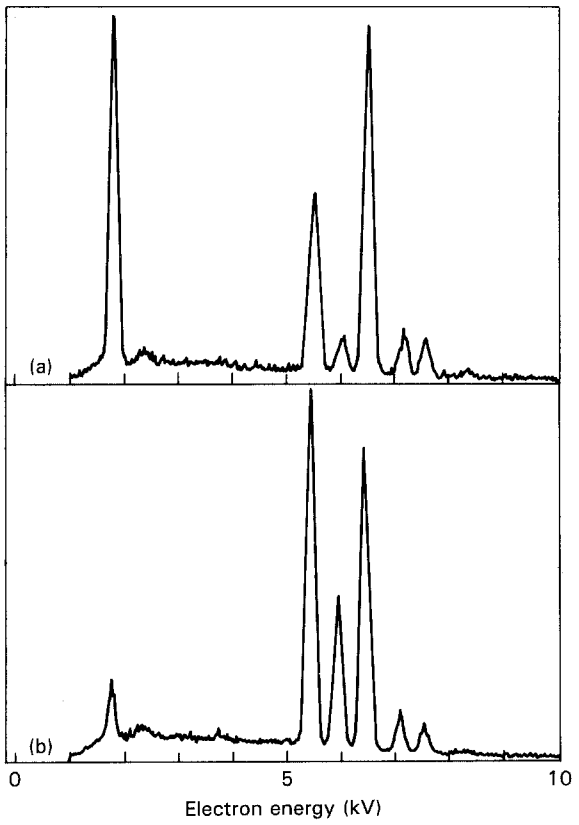

Figure 8 EDX spectra of stainless steel plates heated to 1100 °C in argon gas: (a) stainless steel plate pre-deposited with three layers of SiC at 700 °C and (b) uncoated stainless steel plate.

observed for stainless steel plates coated with SiC in a nitrogen atmosphere although at higher temperatures, this thermal protection was compromised by the tendency of the substrate to form CrN nodules.

3.2. SEM/EDX studies of sol–gel-derived silica coatings on mild steel and stainless steel substrates

To form a "barrier" coating to prevent the metal substrate from reacting with the nascent SiC coating as well as the ancillary role of inhibiting reaction of the metal substrate in the case of stainless steel with the flowing furnace atmosphere (nitrogen), SiO_2 coatings were applied to mild steel and stainless steel substrates. A sol–gel mixture of TEOS (tetra-ethoxy-ortho-silicate) in $EtOH/H_2O$ with glacial acetic acid added as the catalyst was chosen as a non-corrosive solution suitable for deposition on metal substrates to form the silica coatings. In general, the thickness (as judged from %Si/%Fe ratios derived from EDX data) of all sol–gel-derived coatings on stainless steel and mild steel increased as a function of the number of days after mixing of the reagents up to a maximum of 3 days. On the fourth day after mixing of the reagents, any coatings formed by dip-coating the metal substrates into the aged sol–gel coating solution spalled and flaked off immediately after the solvent had evaporated. The SiO_2 coatings on the stainless steel and mild steel substrates were colourless in appearance and were visible by virtue of the protection they imparted to the metal substrates from heating discoloration which was manifest as coloured or black regions in the uncoated regions of the mild steel or stainless steel plates.

3.2.1. SiO_2 Coatings on mild steel plates

Fig. 9 is a scanning electron micrograph of a "1,2" SiO_2 coating on mild steel. Most of the SiO_2 coatings on mild steel exhibited cracks in regions of the layer. Cracking is more common as the thickness of the SiO_2 is increased as a result of dip-coating substrates in an aged sol–gel coating solution. In addition, features which appear as white nodules and multiple strata in the SEM are manifest. In some micrographs, the white features on the micrograph give the impression of material being "squeezed" up between fissures and cracks in the SiO_2 coating, suggesting that a reaction of the iron with the SiO_2 or furnace atmosphere had taken place during the 500 °C heating. In some micrographs, the "squeezed" white material follows fault lines developing in the SiO_2 coating suggesting that the material is responsible for the observed cracking. An EDX analysis of the white nodules and strata on the mild steel plate indicated enhanced FeK_α signals in this area with negligible silicon. This suggests that an iron-rich phase such as Fe_3C has possibly accumulated at the surface of the coated plates. It is possible that the driving force for its formation is contributing to cracking in the SiO_2 coating just as CrN formation appears to contribute to SiC coating cracking on stainless steel.

3.2.2. SiO_2 Coatings on stainless steel substrates

Fig. 10 shows scanning electron micrographs acquired of sol–gel-derived SiO_2 coatings deposited on stainless steel substrates at different stages of the sol–gel coating solution ageing. It was evident from the micrographs (Fig. 10b) that the "1,1" coating was quite thin, given that the scratches and grooves characteristic of the uncoated stainless steel surface (cf.

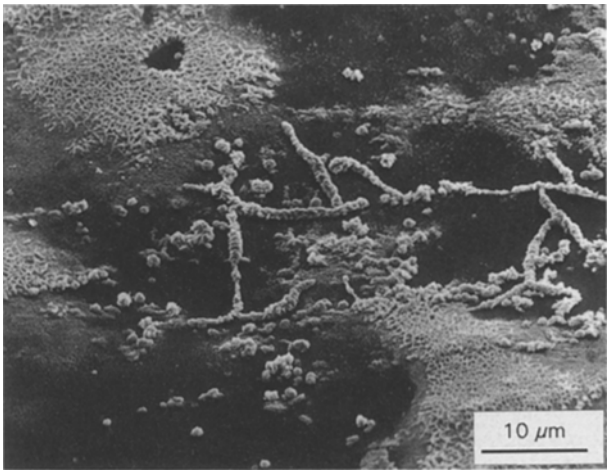

Figure 9 Scanning electron micrograph of a "1,2" SiO_2 layer on mild steel.

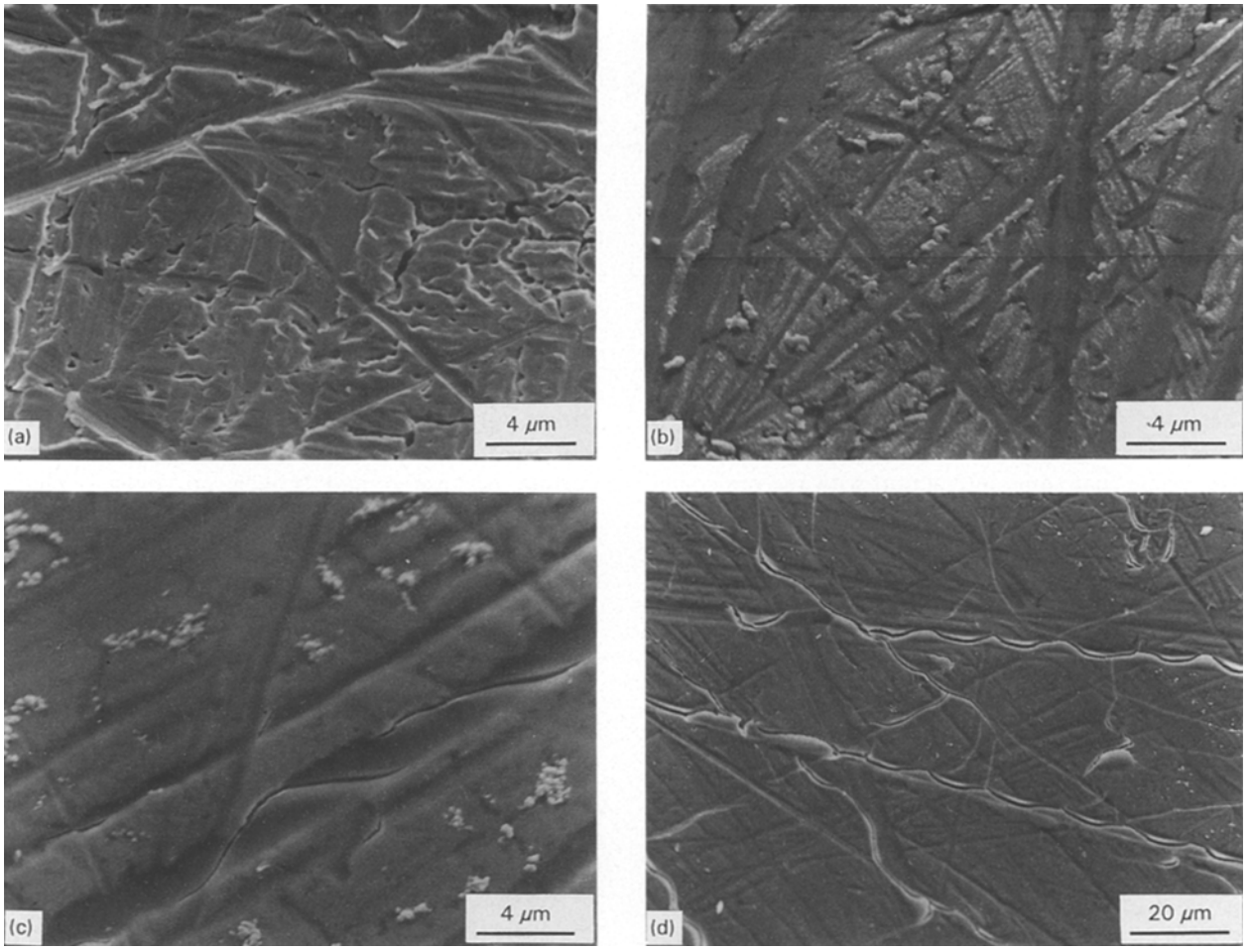

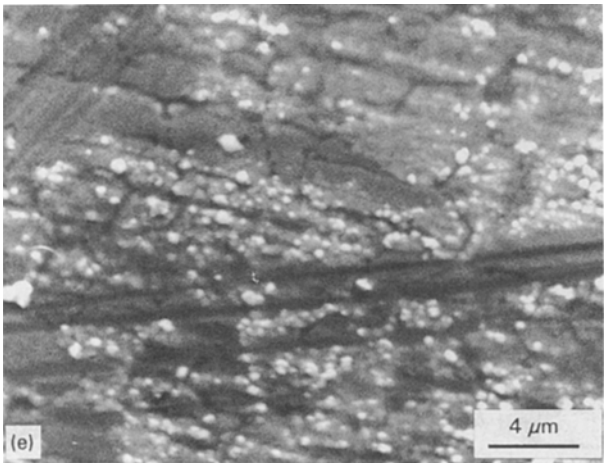

Figure 10 Scanning electron micrographs of SiO_2-coated stainless steel plates: (a) uncoated plate, (b) "1,1" coating, (c) "1,2" coating, (d) "1,3" coating and (e) "1,1,2,2" coating.

Fig. 10a) were still easily visible. However, the appearance of "whitish" nodular deposits on the micrographs was indicative of a coating being present. The thin film was generally crack-free. Micrographs of the "1,2" coating (see Fig. 10c) showed that substrate-associated features were more obscured implying a thicker overlying coating. This observation was in agreement with %Si/%Fe data derived from EDX. The "1,2" coating was beginning to show a few cracks occurring in grooves in the stainless steel substrate. The micrograph of the "1,3" coating (Fig. 10d) showed the SiO_2 coating to be thicker than the "1,2" coating with more cracks. Many of the cracks appeared to run parallel to grooves in the stainless steel substrate. Thus, it appears that as coating thickness increases, cracking is initiated around the scratches existing on the stainless steel surface. Some degree of spalling in the "1,3" SiO_2 coatings was evident on a microscopic scale but only at boundaries between coated and uncoated areas. To the naked eye, the overall "1,3" SiO_2 coating appeared adherent on the plate with no signs of spalling.

Multiple layering of SiO_2 was also examined. A "1,1,2,2" SiO_2 coating was found by SEM to show a preponderance of "white deposits" interspersed around the scratches and grooves in the stainless steel substrate (see Fig. 10e). Spot EDX analysis of the white nodular deposits gave intense SiK_α signals indicating they were composed of SiO_2.

3.3. Deposition of PCS-derived SiC on mild steel and stainless steel plates pre-coated with SiO_2 barrier coatings

3.3.1. Deposition on SiO_2-coated mild steel plates

1100 °C-N_2 pyrolysis of a PCS layer applied to mild steel plates pre-coated with sol–gel derived SiO_2 leads to blackened plates after firing. The adherent black coating possessed a speckly look implying that it was cracked. Indeed, the scanning electron micrograph of

PCS-derived SiC deposited on "1,2" SiO_2-coated mild steel plates (see Fig. 11a) showed large wrinkled looking cracked platelets on the surface. In micrographs of some samples, flat plates which seemed to be embedded in a very roughened substrate surface were apparent. EDX analysis of the platelets confirmed that the plates were silicon-rich and were thus either islands of SiC or SiO_2. The rough areas between the platelets were found by EDX to be iron rich although in other samples SiK_α was detected. EDX also revealed an enhancement in the MnK_α signal relative to the FeK_α signal between the platelets. A low level of manganese is present in the mild steel samples (see Section 2) therefore, the enhanced MnK_α signal could represent manganese migration as observed in stainless steels. It is possible that some interaction with the pre-coated SiO_2 layer is occurring. Also on closer inspection of the micrographs, the phenomenon of substrate material "squeezing up" (as mentioned earlier in relation to SiO_2-coated mild steel plates) between the SiC/SiO_2 platelets was evident. The wrinkles observed in platelets could indicate expansion and shrinkage (i.e. thermal expansion mismatch) between the mild steel substrate and the nascent SiC coating which has led to irreversible damage of the ceramic coating.

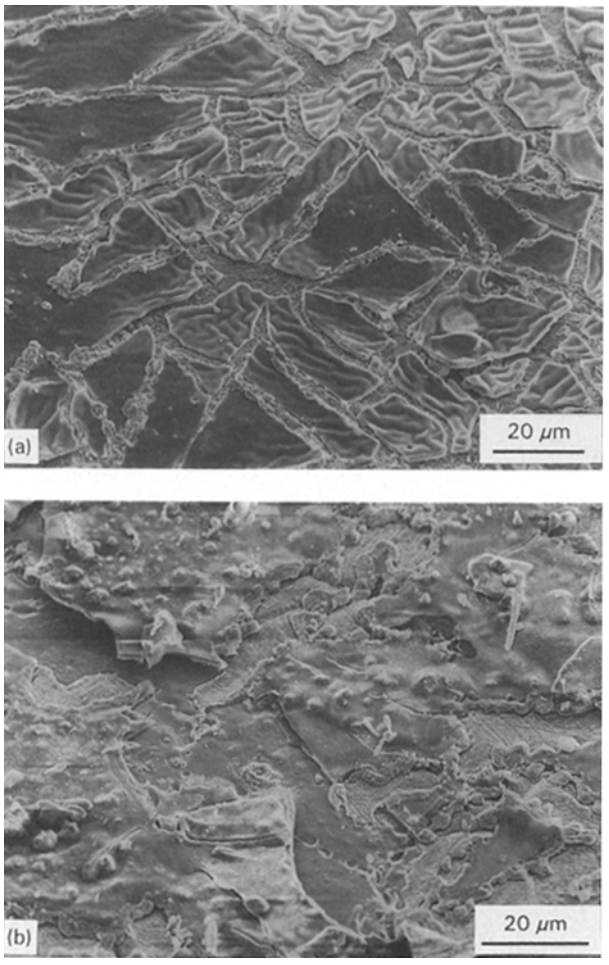

Figure 11 Scanning electron micrographs of SiC deposited on (a) "1,2" SiO_2-coated mild steel plate, and (b) "1,3" SiO_2-coated stainless steel plate.

3.3.2. Deposition on SiO_2-coated stainless steel plates

Deposition of PCS-derived SiC on previously SiO_2-coated stainless steel plates at 1100 °C in nitrogen was also not successful. Fig. 11b shows a scanning electron micrograph of a "1,3" SiO_2-coated stainless steel plate where three coatings of PCS-derived SiC had been overlaid, each formed by separate 1100 °C-N_2 pyrolyses. The surface of the coated plate was considerably roughened and disrupted. The cracked platelets, which were silicon-rich (from EDX measurements) and therefore due to SiC coating, were punctuated with raised nodules most likely due to CrN forming underneath the coating. It is apparent that the SiO_2 film has not fulfilled its intended role as a barrier coating because it had broken up. Indeed, plates which had only been SiO_2-coated and taken up to 1100 °C in nitrogen were found by SEM/EDX to exhibit the characteristic CrN-associated nodules.

3.4. X-ray photoelectron studies of SiC coatings on stainless steel and mild steel substrates

3.4.1. SiC coatings formed at 700–800 °C on stainless steel

The wide-scan X-ray photoelectron spectra of stainless steel plates coated with four layers of SiC formed by repeated dip-coatings and pyrolyses at 700 or 800 °C in nitrogen of PCS layers were practically identical to that reported for SiC on alumina (before sputtering) in Part I of this study [1]. Silicon, carbon and oxygen were the principal components at the surface of the coating. However, this coating behaves differently from the SiC/alumina coating in that the C 1s signal remained even after 30 min argon sputtering. Thus the source of the carbon is not adventitious hydrocarbons but forms part of the bulk coating itself. The C 1s signal shifts to lower binding energies with sputtering. When referenced to the Si 2p peak in the spectra obtained after sputtering, the binding energy position of the C 1s peak was found to occur at 284.6–284.8 eV, which is characteristic of graphite [5]. Thus, the C 1s peak is most probably due to excess carbon remaining after PCS pyrolysis rather than carbide-associated carbon in the amorphous SiC formed at this temperature.

From X-ray photoelectron spectra, it is apparent that the surfaces of the SiC coatings formed at 700 and 800 °C are oxidized as are SiC coatings formed on alumina at 1100 °C [1]. However, unlike the SiC residues formed at 1100 °C where no SiO_2 species were detected by ^{29}Si NMR, the bulk of the graphite-enriched SiC coating formed at 700 °C is expected to contain a small amount of SiO_2 on the basis of ^{29}Si NMR spectra of the bulk residues generated at 700 °C (see earlier).

The Si:C:O ratios for the 700 and 800 °C SiC coatings after 30 min sputtering were 1:0.80:1.65 and 1:0.43:1.9, respectively. Thus for a pyrolysis temperature increase of 100 °C, the level of graphitic carbon in the coatings decreases by over 50%, while the Si:O ratio increases to the value observed for the SiC/alum-

ina system. The coatings, therefore, eventually become covered with SiO_2.

3.4.2. SiC Coatings at 1100 °C on stainless steel

3.4.2.1. Coatings on "SS2" stainless steel substrates. The X-ray photoelectron wide scan spectrum of a stainless steel plate ("SS2") with four layers of PCS-derived SiC formed at 700 °C and subsequently heated to 1100 °C in nitrogen, indicated that the stainless steel had been nitrided (see Fig. 12). Coating formation was shown by SEM to be disrupted by migration of manganese and chromium (to form CrN). These substrate-associated phenomena are reflected by the appearance of N 1s, Cr 2p and Mn 2p peaks in the X-ray photoelectron spectra of the plate at the coating disruptions which expose such components to the surface. The O 1s peak observed in the disrupted coating was intense and may be associated with SiO_2 (from the SiC coating), Mn_2O_3 or possibly Cr_2O_3 emanating from the disrupted stainless steel passive film.

3.4.2.2. Coatings formed on "SS1" stainless steel substrates. X-ray photoelectron spectra were also recorded of SiC deposited on "1,2" SiO_2 pre-coated stainless steel ("SS1") plates. The scanning electron micrograph of this plate showed surface damage by the 1100 °C heating but gave little evidence for coating formation. The XPS revealed that the stainless steel had undergone a significant degree of nitriding at 1100 °C. In addition, Cr 2p, Mn 2p and B1 s signals were observed which have all appeared as a result of heat-induced migration during pyrolysis. Si 2p and Si 2s peaks did not feature strongly in the spectrum. The wide scan spectrum of an uncoated "SS1" plate heated to 1100 °C in nitrogen was almost identical except for much lower silicon levels. The presence of boron and a more intense nitride-associated N 1s peak in the X-ray photoelectron spectrum are features which distinguish the "SS1" stainless steel substrate from the "SS2" substrate.

When narrow scans were recorded over the Si 2p and O 1s regions in the X-ray photoelectron spectrum of the SiC/SiO_2-coated plate, the resultant profiles were very broad, indicating a complex mixture of silicon-containing species. Deconvolution was carried out on these profiles and the resultant data summarized in Table I. For the SiC/SiO_2-coated plate, three peaks can be bandfitted to the Si 2p profile which was shifted upwards in binding energy by charging (see Fig. 13). After correcting for charging, the binding energy positions for the fitted peaks were found to be 101.2, 102.36 and 103.69 eV. The peak at 103.69 eV can be attributed to SiO_2. Binding energies of this magnitude have been observed for the SiO_2 coatings detected on SiC on alumina in Part I as well as for SiO_2 on Nicalon fibres [1, 19]. On the basis of the XPS study on Nicalon fibres [19], the deconvoluted peaks at 101.2 and 102.36 eV could possibly be assigned to SiC and a silicon oxycarbide species (SiC_xO_y), respectively.

Narrow scans over the O 1s region of the SiC/SiO_2 plate also gave broad O 1s profiles indicating a complex oxide mixture on the surface due possibly to silicon oxides, silicon oxycarbides, manganese oxides or chromium oxides. The narrow scan over the O 1s region of the X-ray photoelectron spectrum of uncoated stainless steel ("SS1") plate heated to 1100 °C in nitrogen revealed a somewhat narrower O 1s profile where the higher binding energy peak (at ~ 533 eV) was significantly weaker. This suggests that the higher energy component represented by the fitted peak at 533.3 eV in the SiC/SiO_2-coated plate is mostly due to SiO_2.

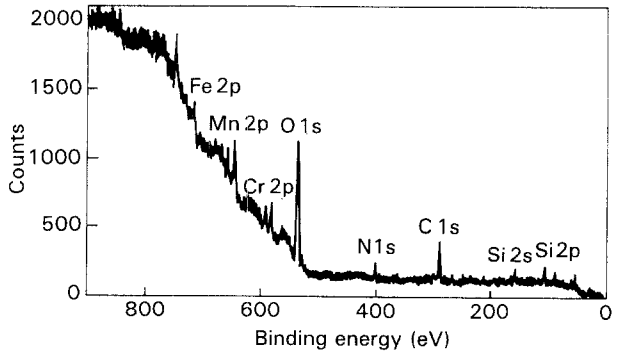

Figure 12 X-ray photoelectron wide scan spectrum of a stainless steel plate pre-deposited with three layers of SiC formed at 700 °C, which had been heated to 1100 °C in nitrogen.

TABLE I Bandfitting data from narrow scans over the Si 2p and O 1s regions of X-ray photoelectron spectra of unsputtered coated and uncoated stainless steel and mild steel plates

System	Region	B.E.[a] (eV)/I[b]/ FWHMM[c]	Assignment
SiC on mild steel/ 1100 °C/N_2	Si 2p	101.6/25.0/1.67	SiC
		103.4/60.0/1.60	SiO_2
		104.2/57.7/1.60	SiO_2
	O 1s	530.0/54.0/1.50	Iron oxides
		532.0/40.0/1.60	
		533.4/92.0/1.65	SiO_2/adsorbed water
Uncoated mild steel plate/1100 °C/N_2	O 1s	530.2/82.0/1.38	Iron oxides and adsorbed water
		530.9/22.0/1.50	
		532.1/18.0/1.65	
SiC on "1,2" SiO_2-coated "SS1" stainless steel	Si 2p	101.1/59.1/1.60	SiC
		102.4/67.0/1.65	
		103.7/73.2/1.67	SiC_xO_y SiO_2
	O 1s	530.4/77.0/1.60	Metal oxides
		531.9/80.0/1.65	
		533.3/75.0/1.65	SiO_2/adsorbed water
Uncoated "SS1" stainless steel/1100 °C/N_2	O 1s	530.2/86.0/1.49	Metal oxides
		531.4/48.4/1.62	
		532.9/22.0/1.67	Adsorbed water

[a] Binding energy (corrected for charging) of fitted peak.
[b] Intensity of fitted band at binding energy quoted.
[c] Full width at half maximum of fitted peak.

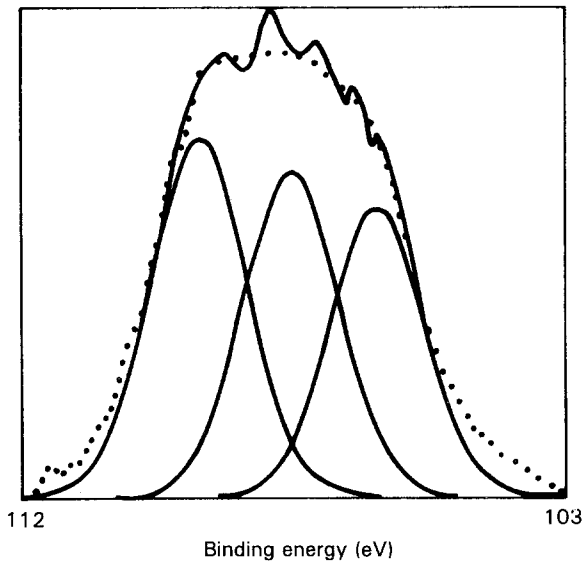

Figure 13 Bandfitted narrow scan profile over the Si 2p region of the X-ray photoelectron spectrum of SiC deposited on an SiO_2-coated stainless steel plate. Binding energy positions are shifted upwards by 4.61 eV due to charging.

3.4.3. Formation of SiC coatings on mild steel plates at 1100 °C

XPS examination of a mild steel plate where PCS was applied directly to its surface followed by 1100 °C-N_2 pyrolysis revealed iron, silicon and oxygen to be the principal surface components. There is a possibility that silicon has chemically combined with surface iron. Iron is known [20, 21], to react with SiC to form Fe_3C or iron silicides. The narrow scan over the Si 2p region of the X-ray photoelectron spectrum of the plate gives a Si 2p profile with a distinct asymmetry towards lower binding energies. Three Si 2p peaks can be fitted to the experimental profile (see Table I) with binding energies (corrected for charging) at 101.6, 103.38 and 104.22 eV. The fitted peak at 101.6 eV exhibits a binding energy typical of SiC [18, 21]. Although X-ray photoelectron data appear to be lacking for these compounds, the fitted peak at 101.6 could be due to iron silicides or possibly FeSiC. The fitted peaks with binding energies at 103.38 and 104.22 eV are probably associated with SiO_2-type species implying that the bulk of the silicon signal in the spectrum is due to surface SiO_2 which may have formed from interaction of the PCS (or nascent SiC) with the iron surface oxides. This is supported by the narrow scan over the O 1s region of the X-ray photoelectron spectrum of the SiC on iron plate (Fig. 14a) which shows an intense peak that is found to occur at the charging-corrected binding energy of 533.41 eV. This peak reduced in intensity after sputtering and so is mostly due to adsorbed water. The weaker peak remaining is probably due to SiO_2-associated oxygen. The lower binding energy peak which occurs at 530.0 eV (after correction for charging) has been assigned to iron oxides. Indeed, the narrow scan of the O 1s peak in the X-ray photoelectron spectrum of an uncoated mild steel plate (Fig. 14b) heated to 1100 °C in nitrogen gives an intense O 1s peak which after charge correction is found to be centred at ~ 530 eV

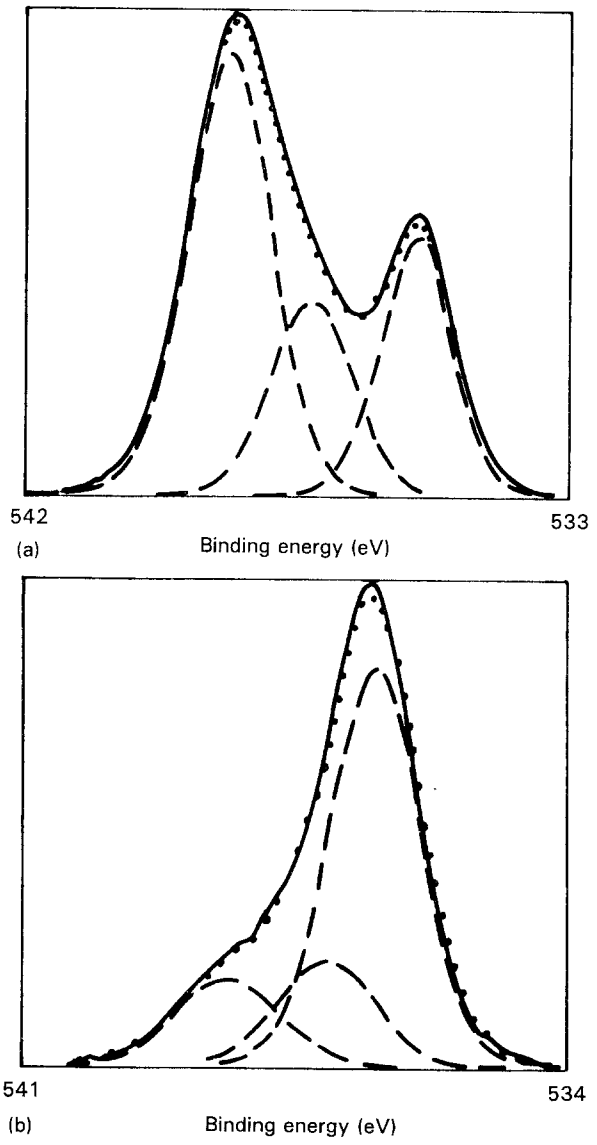

Figure 14 Bandfitted narrow scan profile over the O 1s region of the X-ray photoelectron spectra of (a) SiC deposited directly on to mild steel plate by 1100 °C-N_2 pyrolysis of an applied PCS layer (binding energies are shifted by + 5.22 eV due to charging), and (b) uncoated mild steel plate in nitrogen (binding energies are shifted by + 6.21 eV due to charging).

with much lower intensity fitted peaks in the higher binding energy end of the spectrum (Fig. 14b) where SiO_2-associated oxygen and adsorbed water occur. This confirms the assignment of the 530 eV (charge-corrected) peak in Fig. 14a to an iron oxide species.

3.5. Rutherford backscattering spectra of SiC coatings on stainless steel plates

Fig. 15 shows RBS spectra obtained from an uncoated "SS2" stainless steel plate and an "SS2" plate coated with four layers of SiC formed at 700 °C. The RUMP simulation profile of an infinitely thick layer of stainless steel (SS2) using the EDX-derived percentages of iron, chromium, nickel, manganese and silicon, gave a very close fit to the RBS profile obtained for uncoated stainless steel (see Fig. 15). In the RBS spectrum of the SiC-coated stainless steel, it is immediately evident that a distinct shift to lower energy in the stainless steel RBS profile occurs as a consequence of the

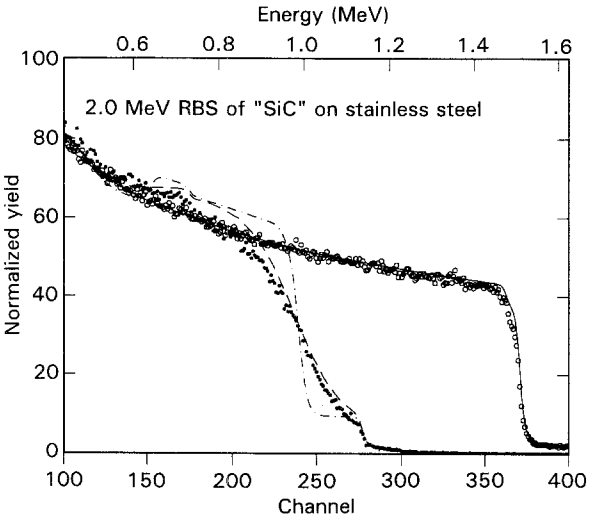

Figure 15 Rutherford backscattering spectra of (○) uncoated "SS2" stainless steel and (●) stainless steel coated with PCS-derived SiC deposited by 700 °C pyrolysis. For the uncoated stainless steel, the solid superimposed RUMP-simulated spectrum is calculated assuming a 5000 nm layer of stainless steel consisting of Si (0.451), Mo (2.028), Cr (15.970), Mn (1.455), Fe (68.235), and Ni (11.861) where bracketed values refer to elemental per cent values. For the SiC-coated stainless steel, two RUMP simulations are superimposed assuming a 7×10^{18} at cm^{-2} $SiOC_{1.5}$ coating and a straggling factor of 1. (– – –) Simulation with "fuzzing" over 1.35×10^{18} at cm^{-2} of the $SiOC_{1.5}$ layer included; (— · —) simulation which does not include "fuzzing".

deposition of the SiC coating. The energy difference between the onset of the RBS profiles for the uncoated and coated stainless steel samples was used to deduce an approximate atom thickness of 7×10^{18} atoms cm^{-2} for the SiC coating. If it is assumed that the "SiC" coating consists entirely of $SiOC_{1.5}$, then a thickness value (in nanometres) can be computed from the average atomic mass of $SiOC_{1.5}$ and assuming a density of $\sim 3.0\ g\,cm^{-3}$ (being intermediate between the density of glass (SiO_2, 2.4–2.8 $g\,cm^{-3}$) and crystalline SiC (3.2 $g\,cm^{-3}$)). This gives a thickness of 686 nm which agrees well with the EDX-derived thickness of 630 nm (see above).

Two RUMP simulations have been superimposed on the RBS spectrum of SiC-coated stainless steel to show the effect of "fuzzing" on goodness of fit of the simulated profiles to the experimental data (see Fig. 15). In both simulations, the composition of the coating is assumed to be $SiOC_{1.5}$ with atom thickness 7×10^{18} atoms cm^{-2} which overlies a second infinitely thick (5000 nm) stainless steel layer. The composition of $SiOC_{1.5}$ is believed to be a reasonable composition for the "SiC" layer because both SiO_2 and graphitic carbon were detected in the XPS spectra of the coated stainless steel plates (see above). The simulation shown (– – –) is calculated with fuzzing over 1.35×10^{18} atoms cm^{-2} of the $SiOC_{1.5}$ layer and gives the better fit. The simulation computed without fuzzing (— · —) introduced into the $SiOC_{1.5}$ coating layer gives a much worse fit to the experimental data. It is obvious that the "fuzzing" is simulating the inherent roughness of the stainless steel interface with the deposited SiC coating. However, it is noticeable that the "fuzzed" simulation used did not produce an optimum fit for this particular coating system. This is believed to be caused by compositional inhomogeneity due to chemical mixing at the stainless steel/SiC interface which is not unexpected given that SEM/EDX studies have demonstrated that the stainless steel substrate is very reactive towards the ceramic coating.

3.6. Microhardness measurements on SiC coatings formed at 800 °C on stainless steel substrates

The microhardness data for stainless steel plates coated with SiC formed by 800 °C-N_2 pyrolysis of PCS layers are summarized in Table II. SiC coatings on stainless steel exhibit hardness values which are approximately 50% lower than those measured by the UMIS-200 for SiC coatings formed on alumina plates at 1100 °C [1]. Hardness values appear very consistent for loads less than or equal to 20 mN where the depth of penetration into the coating is less than the SiC coating thickness which was estimated to be $\sim$ 580 nm (see earlier). For a load of 50 mN, where the measured depth of penetration is 773 nm, the hardness value shows a significant decrease to 3.78 GPa. Comparison with hardness measurements carried out on uncoated, unheated stainless steel shows that penetration through the SiC coating has occurred at this loading because hardness values are closer to those expected for stainless steel (2.40–3.67 GPa). The hardness values determined for the blank stainless steel plate show a considerable degree of scatter because of the uncoated stainless steel surface is somewhat rougher than the coated specimens. This introduces scatter into indentation meas-

TABLE II Summary of microhardness measurements[a] performed by the UMIS-2000 on uncoated and SiC-coated[b] stainless steel plates

Specimen	Load (mN)	Hardness (GPa)	Modulus (GPa)	Measured penetration depth (nm)[c]
Uncoated	50	3.55	179.0	779
stainless	100	2.72	173.0	1237
steel plate	200	2.44	203.0	1822
	500	2.37	199.0	2971
SiC coating on	5	5.49	59.3	228
stainless steel	10	5.48	70	324
formed at 800 °C	20	5.51	83	455
	50	3.78	114.9	773

[a] Measurements represent the average of six to ten individual load–unload plots at the load value (in mN) specified.
[b] The stainless steel plate was coated with four layers of amorphous SiC applied by separate dip-coatings of an "SS1" stainless steel plate in a PCS/hexane coating solution followed by 800 °C-N_2 pyrolyses.
[c] This represents the actual depth of penetration but the analysis of the load–unload data works with an adjusted total penetration value which is the measured penetration depth plus a contribution made by two components: a small initial penetration caused by the contact force when the indentor comes into contact with the sample and (2) a component due to the tip curvature which causes the contact diameter to be larger than measured.

urements by the UMIS-2000. A similar problem was observed with microhardness measurements of uncoated alumina plates [1]. However, overall the coating of stainless steel by the SiC at 800 °C gives a layer which is harder than the stainless steel alone. However, this coating is still easily scratched off.

Earlier, it was shown by XPS that graphite arising possibly from excess carbon remaining after the incomplete pyrolysis of the PCS polymer at 800 °C was present in the SiC coating. It is possible that the graphite remaining leads to softer coatings. As the firing temperature increases, the graphite is probably lost (as CO) [23] and the coating hardens as a result.

A search for the indentations by SEM revealed that the indented areas showed small triangular depressions in the coated plate with no evidence of coating damage around the depressions.

4. Conclusions

Ceramic coatings derived from pre-ceramic polymer pyrolysis present problems when applied to metal substrates. Crack-free amorphous SiC coatings can be formed on stainless steel substrates from PCS pyrolysis only at temperatures not exceeding 800 °C. On the other hand, SiC coatings formed on mild steel plates are cracked when formed at 700 °C.

The surfaces of SiC coatings formed at a temperature of 800 °C on stainless steel plates are found by XPS to be covered in SiO_2 and contain graphite. Rutherford backscattering spectrometry indicates a layer consisting on average of $SiOC_{1.5}$ with possible chemical mixing of coating and substrate components at the interface between the two.

Microhardness measurements on a SiC coating formed at 800 °C indicates hardness values of only approximately 50% of those values measured for SiC coatings formed on alumina substrates at 1100 °C. The lower microhardness values are a consequence of the lower pyrolysis temperature which leaves XPS-detectable levels of graphitic excess carbon from the pre-ceramic polymer in the surfaces of the coatings. The measured hardness values are only slightly higher than hardness values of uncoated stainless steel plates measured by the same method.

When pyrolysis temperatures exceed 800 °C, the SiC coating on stainless steel cracks which worsen with increasing pyrolysis temperature. For stainless steel plates pyrolysed in nitrogen, this cracking has been shown by EDX analysis to be caused initially by chromium and manganese-enriched protrusions emerging at the substrate surface which disrupt the SiC layer. As the temperature is increased, a combination of factors involving CrN formation, manganese migration and thermal expansion mismatch is believed to cause the more serious disruption in coatings.

Sol–gel-derived SiO_2 coatings have been applied to mild steel and stainless steel plates prior to PCS application and 1100 °C pyrolysis. Although the SiO_2 coatings, *per se*, inhibit heat-induced discolouring on mild steel and stainless steel plates at 500 °C, they do not function as effective barrier coatings preventing the disruption wreaked upon SiC coatings formed on the metal substrates at pyrolysis temperatures of 1100 °C.

Acknowledgements

The authors thank the foundation for Research, Science and Technology for the awarding of a post-doctoral fellowship to M.R.M., Mrs Kay Card, Superconducting Team in Industrial Research Ltd, for the recording of the numerous electron micrographs and EDX analyses required for this study, Dr Ian Vickridge, Institute of Geological and Nuclear Sciences, Lower Hutt, for performing the Rutherford backscattering spectrometry, and Dr Michael Swain for carrying out the ultramicrohardness measurements on the UMIS-2000 instrument at the CSIRO Division of Applied Physics, NSW, Australia. Richard Meinhold is thanked for recording NMR spectra of the PCS-derived residues.

References

1. M. R. MUCALO, N. B. MILESTONE, I. C. VICKRIDGE and M. V. SWAIN, *J. Mater. Sci.* **29** (1994) 0000.
2. S. YAJIMA, T. SHISHIDO, H. KAYANO, Y. HIGASHIGUCHI and T. AMAMO, *ibid.* **12** (1977) 1834.
3. D. SEYFERTH, N. BRYSON, D. P. WORKMAN and C. A. SOBON, *J. Am. Ceram. Soc.* **74** (1991) 2687.
4. E. J. A. POPE and J. D. McKENZIE, *J. Non-Cryst. Solids* **87** (1986) 185.
5. D. BRIGGS and M. P. SEAH (eds.), in "Practical Surface Analysis by Auger and X-ray Photoelectron Spectroscopy" (Wiley, New York, 1983).
6. L. R. DOOLITTLE, *Nucl. Instrum. Meth.* **B9** (1985) 334.
7. "RUMP Users Manual" (Computer Graphics Services, 52 Genung Circle, Ithaca, New York 14850, USA).
8. J. S. FIELD, *Surf. Coat. Technol.* **36** (1988) 817.
9. T. J. BELL, A. BENDELI, J. S. FIELD, M. V. SWAIN and E. G. THWAITE, *Metrologia* **28** (1991/92) 463.
10. T. TAKI, M. INUI, K. OKAMURA and M. SATO, *J. Mater. Sci. Lett.* **8** (1989) 918.
11. M. R. MUCALO, N. B. MILESTONE and I. W. M. BROWN, submitted to *J. Amer. Ceram. Soc.*
12. C. J. SMITHELL (ed.), "Metals Reference Book" (Butterworths, London, 1976).
13. J. F. LYNCH (ed.), "Engineering Property Data on Selected Ceramics", Vol. 2, (Metals and Ceramics Information Centre, Battelle, Columbus Laboratories, OH, 1979) p. 23.
14. K. KANAYA and S. OKAYAMA, *J. Phys. D Appl. Phys.* **5** (1972) 43.
15. R. D. WILLENBRUCH, C. R. CLAYTON, M. OVERSLUIZEN, D. KIM and Y. LU, *Corros. Sci.* **31** (1990) 179.
16. R. A. HIGGINS, "Materials for the Engineering Technician" (Hodder and Stoughton, London, 1984) p. 164.
17. M. CAVALLINI, F. FELLI, R. FRATESI and F. VENIALI, *Werkstoffe Korrosion* **33** (1982) 386.
18. P. MARCUS and M. E. BUSSELL, *Appl. Surf. Sci.* **59** (1992) 7.
19. P. SCHRECK, C. VIX-GUTERL, P. EHRBURGER and J. LAHAYE, *J. Mater. Sci.* **27** (1992) 4243.
20. K. M. GEIB, C. W. WILMSEN, J. E. MAHAN and M. C. BOST, *J. Appl. Phys.* **61** (1987) 5299.
21. Y. MIZOKAWA, S. NAKANISHI and S. MIYASE, *Jpn J. Appl. Phys.* **28** (1989) 2570.
22. T. A. CARLSON, "Photoelectron and Auger Spectroscopy" (Plenum Press, New York, 1975) p. 355.
23. P. L. COUSTUMER, M. MONTHIOUX and A. OBERLIN, *J. Eur. Ceram. Soc.* **11** (1993) 95.

Received 25 June 1993
and accepted 19 January 1994